Manuscript submitted to **Biophysical** *Journal*
Article

Fabrication and electromechanical characterization of free-standing asymmetric membranes

P. Liu[1,†], O. Zabala-Ferrera[1,†], and P. J. Beltramo[1,*]

*

ABSTRACT All biological cell membranes maintain an electric transmembrane potential of around 100 mV, due in part to an asymmetric distribution of charged phospholipids across the membrane. This asymmetry is crucial to cell health and physiological processes such as intracell signaling, receptor-mediated endocytosis, and membrane protein function. Experimental artificial membrane systems incorporate essential cell membrane structures, such as the phospholipid bilayer, in a controllable manner where specific properties and processes can be isolated and examined. Here, we describe a new approach to fabricate and characterize planar, free-standing, asymmetric membranes and use it to examine the effect of headgroup charge on membrane stiffness. The approach relies on a thin film balance used to form a freestanding membrane by adsorbing aqueous phase lipids to an oil-water interface and subsequently thinning the oil to form a bilayer. We validate this lipid-in-aqueous approach by analyzing the thickness and compressibility of symmetric membranes with varying zwitterionic DOPC and anionic DOPG content as compared to previous lipid-in-oil methods. We find that as the concentration of DOPG increases, membranes become thicker and stiffer. By controlling the lipid composition in the aqueous compartments on either side of the oil within the thin film balance, asymmetric membranes are then examined. Membrane compositional asymmetry is qualitatively demonstrated using a fluorescence quenching assay and quantitatively characterized through voltage-dependent capacitance measurements. Stable asymmetric membranes with DOPC on one side and DOPC/DOPG mixtures on the other were created with transmembrane potentials ranging from 10 to 25 mV. Introducing membrane charge asymmetry also increases the stiffness of the membrane. These initial successes demonstrate a viable pathway to quantitatively characterize asymmetric bilayers that can be extended to accommodate more complex membrane processes in the future.

SIGNIFICANCE A defining characteristic of the cell membrane is asymmetry in phospholipid composition between the interior and exterior bilayer leaflet. Although several methods have been used to artificially create membranes with asymmetry, there has not been extensive characterization of the impact of asymmetry on membrane material properties. Here, a technique to fabricate free-standing asymmetric membranes is developed which facilitates the visualization and electromechanical characterization of the bilayer. Asymmetry in anionic phospholipid concentration is quantified by measurements of membrane capacitance at varying voltages, which also allows for determination of the membrane compressibility. This method represents an advance in the development of artificial biomembranes by reliably creating phospholipid bilayers with asymmetry and facilitates the interrogation of more complex biological processes in the future.

INTRODUCTION

As the barrier between the cell's interior and its outside environment, the cell membrane is a key interface in biological systems. Consequently, it has been a high priority for many years to understand the components of the cell membrane, and in particular to decipher the role of the phospholipid bilayer in myriad biological processes occuring in the cell. (1–5). In order to better understand the contribution of membrane structure and composition on the numerous functions the cell membrane performs, an array of artificial biomembrane systems have been employed to control experimental parameters in order to extract quantitative

understanding of membrane material properties. Systems that are widely in use include vesicle based techniques such as liposomes and giant unilamellar vesicles (GUVs)(6, 7) and planar systems such as droplet interface bilayers (DIBs)(8–10), supported lipid bilayers (SLBs)(11, 12), and black lipid membranes (BLMs)(13, 14). These systems have been used to conduct numerous studies characterizing the biophysical properties of lipid bilayers, such as the determination of membrane bending rigidity via micropipette aspiration (15, 16), optical flicker spectroscopy (17, 18) or small-angle x-ray scatting (19, 20), as well as the electromechanical properties of DIBs (21) or BLMs (22–24). The majority of this work has been performed using symmetric membranes, where each leaflet has the same phospholipid composition.

However, the cell membrane possesses an asymmetric phospholipid composition where, in particular, the interior leaflet of the cell is enriched with negatively charged phospholipids compared to the exterior leaflet (25–30). This membrane charge distribution drives interaction with macromolecules at interface (31), dictates biological processes such as vesicle budding (32), controls the conformation of membrane proteins (33, 34), and becomes altered when cells undergo cancerous transformation (35–42). As a result, there has been a recent surge of interest in fabricating asymmetric model systems for the systematic study of the role of phospholipid asymmetry in biological systems. The techniques described above have all recently been applied to asymmetric membranes. For example, asymmetric vesicles and GUVs can be formed using cyclodextrin-mediated lipid exchange (43, 44), from inverted emulsion transfer (45, 46), or by using a jet-flow method (47). Asymmetric SLBs formed from vesicle adsorption(48), Langmuir-Blodgett techniques (49), and cyclodextrin-mediated exchange (50) have shown interesting domain coupling between leaflets. The DIB approach to creating membranes can readily accomodate leaflet asymmetry (51, 52), and free-standing asymmetric BLMs may also be formed using the Montal-Mueller technique(53). However, there remains a dearth of systematic studies quantifying the relationship between compositional asymmetry and membrane material properties, with the notable exception of recent GUV experiments that determined that the bending moduli of asymmetric membranes was 50% greater than their symmetric counterparts (54, 55).

We have recently developed a microfluidic platform to create planar, freestanding, large area model biomembranes (LAMBs) which allow for characterization of membrane elasticity and compressibility(56–58). In this work, we extend the LAMB platform to fabricate asymmetric phospholipid membranes and focus on the effect of changes headgroup charge on the membrane Young's modulus. Previously, only symmetric membranes were able to be formed by this method because it relied on lipids suspended in an oil solvent (lipid-in-oil). To create membrane asymmetry, we first establish the use of lipids suspended in independent aqueous buffers on either side of the membrane (lipid-in-aqueous). We validate the lipid-in-aqueous approach by comparison to the lipid-in-oil method using symmetric membranes formed from binary mixtures of zwitterionic and anionic phospholipids. For the asymmetric studies, we start by qualitatively demonstrating the fabrication of an asymmetric bilayer using a fluorescence quenching assay. We then quantitatively characterize the offset potential and increase in bilayer compressibility that occurs upon introducing membrane charge asymmetry. The results demonstrate the ability of this platform to quantitatively characterize asymmetric membranes using this new fabrication approach.

MATERIALS AND METHODS

Materials

The phospholipids 1,2-dioleoyl-sn-glycero-3-phosphocholine (DOPC), 1,2-dioleoyl-sn-glycero-3-phospho-(1'-rac-glycerol) sodium salt (DOPG), and 1,2-dioleoyl-sn-glycero-3-phosphoethanolamine-N-(lissamine rhodamine B sulfonyl) ammonium salt (DOPE-Rh) were obtained from Avanti Polar Lipids. Sodium chloride (NaCl), calcium chloride ($CaCl_2$), sodium bicarbonate ($NaHCO_3$), hexadecane and octadecyltrichlorosilane (OTS) were purchased from Fisher Scientific. All aqueous solutions are prepared using ultra-pure water (Milli-Q, Millipore-Sigma) and are filtered with a 0.2 μm pore filter. Before use, hexadecane is filtered though an 0.2 μm aluminum oxide mesh. QSY-7 succinimidyl ester was obtained from Life Technologies Corporation.

Symmetric Bilayer from Oil Phase

Lipid mixtures are prepared from stock dilutions in chloroform and dried in scintillation vials under nitrogen. The vials are then placed under high vacuum (~5mbar) overnight so any residual chloroform is removed. To fabricate symmetric bilayers in the lipid-in-oil fashion, the dried lipids are resuspended in oil (*n*-hexadecane) at a concentration of 2.5 mg/mL. The lipid solution is then sonicated for at least 2-4 hours with additional sonication before use in an experiment. The bikewheel chip used in the LAMB platform is custom ordered from Micronit Microfluidics. Before use, the bikewheel chip is functionalized using 1mM OTS in hexadecane to make the interior channels hydrophobic. The chip is then plasma cleaned for 5 seconds to remove part of the functionalization on the exterior of the chip. The experimental setup requires (i) a differential pressure transducer, (ii) a syringe pump, (iii) a sample holder with fluid chambers, and (iv) the bikewheel microchip, as shown in Figure 1C. The bikewheel microchip is loaded with the lipids suspended in oil then installed in the sample holder. Vacuum grease seals the glass microfluidic chip to the sample chamber, allowing for the chemical and electronic isolation of the chambers on either

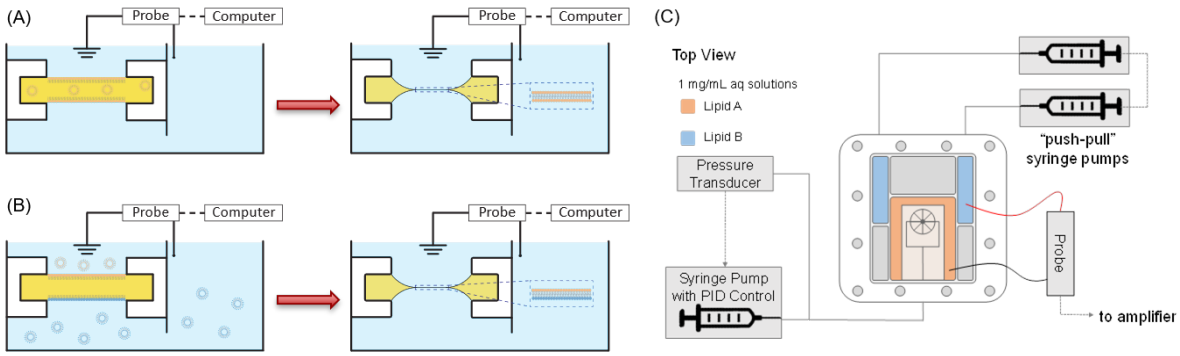

Figure 1: Schematic of the procedure to form bilayers from a) lipid-in-oil and b) lipid-in-aqueous phase by thinning a thick oil film in a microfluidic device. C) The lipid-in-aqueous approach allows for creating asymmetric membranes by integration with microfluidic syringe pumps.

side of the chip. PTFE tubing is used to connect the capillary tube leading to the microchannels in the chip to a syringe pump regulated by a pressure transducer. A salt buffer is prepared with 150mM NaCl, 2mM CaCl, and 0.2 mM $NaHCO_3$. This buffer is loaded into the fluid chambers above and below the microfluidic chip. Pressure on the capillary tube is increased to create a thick oil film at the aperture of the bikewheel chip, then the pressure is lowered so that oil will slowly drain and the thick film will thin. This process is monitored with an inverted microscope (Nike Eclipse Ti2) with a 10x long working distance objective and high speed camera (Hamamatsu ORCA-Flash 4.0). As the film thins, interference fringes appear, and the nucleation and growth of a black lipid film is observed. The area of this bilayer can be controlled depending on the pressure set on the syringe pump. A schematic of the thinning of the thick film into a lipid bilayer is shown in Figure 1A.

Bilayer Fabrication from Aqueous Phase

To prepare a bilayer using the lipid-in-aqueous fabrication approach, the dried lipids are suspended in the prepared buffer solution at a concentration of 0.1 wt%. The aqueous solution is then sonicated in a water bath for 6-8 hours to convert the lipids into liposomes. To create a bilayer, the microfluidic chip is loaded with pure hexadecane instead of a lipid-oil mixture. The compartments in the sample holder are then loaded with the aqueous lipid solution. A thick film of hexadecane is formed in the microfluidic chip and left for 30 minutes to allow lipids to adsorb to the oil-aqueous interface. A bilayer is then formed in the same fashion as above by thinning the film. To generate an asymmetric bilayer, the channels are first loaded with buffer sans lipid, then a thick oil film is formed. With the thick oil film in place, a dual push-pull syringe pump system is used to exchange the aqueous channel below the thick oil film with lipid solution B. The top channel is then exchanged with lipid solution A using micropipettes. After the solution exchanges are completed, the system is given around 30 minutes to equilibrate, then the pressure on the capillary is dropped so that the oil can drain and an asymmetric bilayer will form. A representation of this process is shown in Figure 1B and 1C.

Capacitance Characterization

To characterize the bilayers electronically, a patch clamp amplifier system (HEKA) is used with a pulse generator file to automate the voltage application and data collection process. In a typical experiment, alternating pulses of positive and negative voltage ranging from an amplitude of 25 mV to 200 mV are applied in 1 second pulses with a 2 second "off" pulse in between voltage steps. During capacitance characterization, the bilayer is simultaneously imaged at 10 FPS so that the area of the bilayer can be matched to the measured capacitance across the bilayer. A custom MATLAB script is implemented to accurately determine the membrane area. An example set of this data is shown in Figure 2. Membrane area and capacitance data is used to calculate the voltage dependent hydrophobic thickness of the bilayer, which can be used to quantify the membrane Young's modulus (compressibility), and in addition calculate the offset voltage for membranes with charge asymmetry, as explained below.

Fluorescence Quenching Assay

To demonstate the formation of an asymmetric bilayer, a fluorescence assay was conducted by adding QSY-7, a black hole amine-based quencher, to membranes formed with 1 mol% DOPE-Rh. Three assays were run- introducing the QSY-7 quencher to one side of a fluorescently symmetric bilayer and the two sides of an asymmetric bilayer with fluorescent headgroup lipid

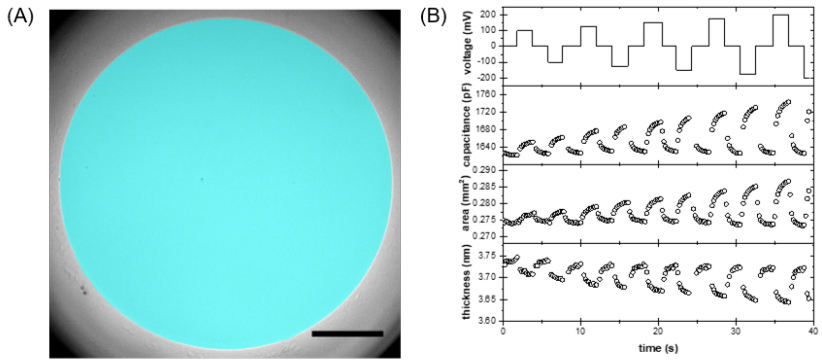

Figure 2: a) Image of a formed bilayer with the membrane area detected by image processing false colored in blue. Scale bar is 100 μm B) Exemplary experiment applying a voltage sweep while measuring membrane area, capacitance, and thickness.

only on one side. The fluorescence was monitored before and after quench and measured using ImageJ in ten separate areas on each bilayer image to obtain ten fluorescent intensities. These intensities were then averaged and scaled by the pre-quench intensities to obtain scaled fluorescent intensities before and after quench.

RESULTS AND DISCUSSION

Comparison between Lipid-in-Oil and Lipid-in-aqueous Fabrication Methods

Previous work performed with the LAMB platform created bilayers from lipids suspended in an oil phase, which was effective in controlling the phospholipid composition in symmetric bilayers (57) but could not produce asymmetric membranes since the lipids would adsorb to both sides of the oil-aqueous interface. To generate membrane asymmetry with this platform, it is necessary to isolate the aqueous compartments on either side of the oil interface and introduce phospholipids from the aqueous phase. We first validate this fabrication approach by analyzing the thickness and compressibility of symmetric membranes with the same composition formed from either the original lipid-in-oil approach or the new lipid-in-aqueous method using binary DOPC/DOPG bilayers. Visually, there is no difference in bilayer formation in either method- after the thick oil film thins and interferometric fringes appear the nucleation and growth of a circular black lipid membrane follows, whose area can be controlled by the capillary pressure in the microfluidic chip. We do find that it is necessary to ensure that there is an adequate concentration of lipids at the oil-aqueous interface before thinning for successful bilayer formation to occur. With lipids suspended in oil at a concentration of $0.3 - 0.6$ wt% , this happens relatively rapidly and the bilayer may be formed almost immediately after creating the thick oil film. However, with lipids suspended in the aqueous phase at a lower concentration of 0.05 wt% to 0.2 wt%, it is necessary to wait at least 30 minutes to ensure an adequate interfacial concentration, or a bilayer will

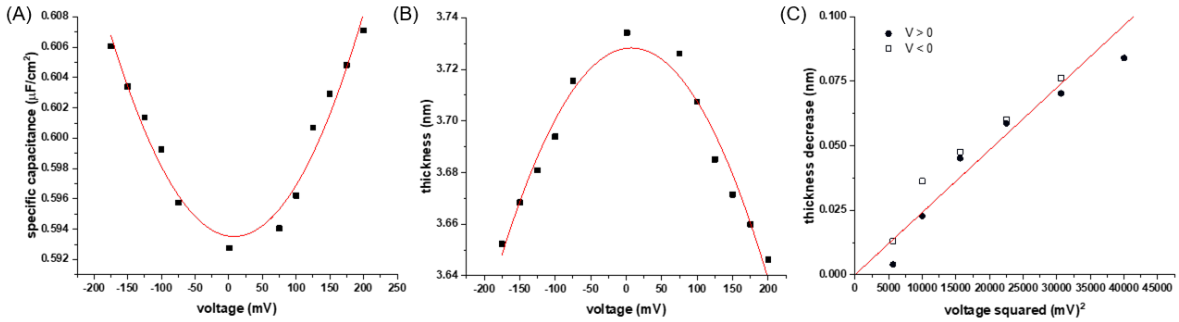

Figure 3: a) Specific capacitance and b) thickness for a DOPC bilayer formed from the lipid-in-oil approach. The bilayer compresses symmetrically with voltage, as shown in c). The membrane Young's modulus is inversely related to the slope of the thickness vs. V^2 relationship.

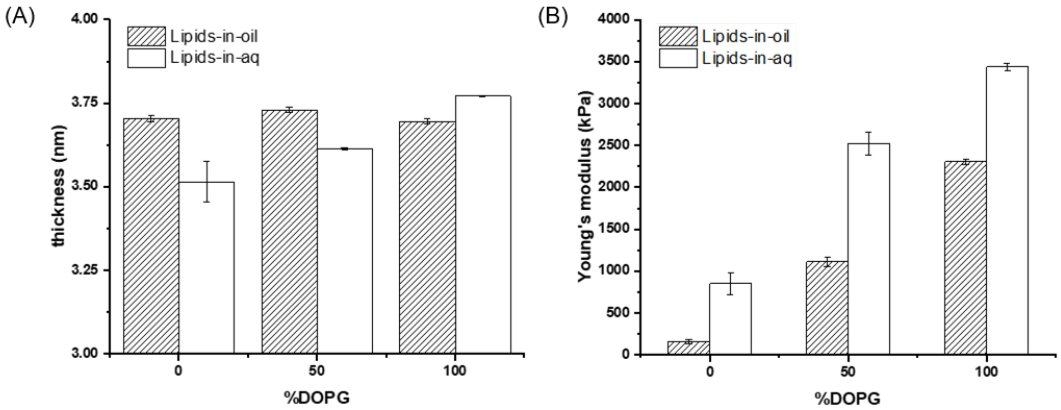

Figure 4: A) The dependence of hydrophobic membrane thickness on DOPC/DOPG concentration and the method of bilayer fabrication. B) Increasing DOPG content stiffens membranes, while membranes formed from the aqueous phase are more stiff than their oil counterparts.

not nucleate upon thinning.

Once formed, membranes are characterized using the voltage pulse method described above. By lining up capacitance measurements with area measurements derived from simultaneous imaging, we calculate the specific capacitance and thickness for each applied voltage, as shown in Figure 3A-B. As expected for symmetric membranes (24), the specific capacitance and thickness of the membranes are quadratic with respect to voltage and centered at zero. The membrane Young's modulus is determined from fitting the thickness decrease-voltage relationship,

$$\Delta d = \frac{C_m V^2}{2E_\perp}, \tag{1}$$

where Δd is the decrease in thickness from the static thickness, C_m is the static membrane specific capacitance, V is the applied voltage, and $E_\perp$ is the Young's modulus (Figure 3C). We found minimal dependence of static thickness with DOPG content in a DOPC-DOPG binary mixture using the lipid-in-oil approach, however, the hydrophobic thickness consistently increased when adsorbing lipids from the aqueous phase (Figure 4A). It is possible membranes formed from the lipid-in-aqueous phase possess less residual oil in the resulting bilayer, causing decreased thicknesses and the compositional dependence of thickness to be clearer. It has previously been shown that membranes formed from hexadecane have larger thickness than their solvent-free counterparts due to residual oil molecules remaining in the membrane(21, 57), which has been estimated to be ~36% using molecular dynamics simulations (59). The increase in thickness with DOPG concentration is likely due to anionic DOPG introducing increased electrostatic repulsion between headgroups on opposing leaflets, which has also been observed in the solvent-free thickness of bilayers measured with small angle x-ray scattering (SAXS)(60, 61).

The Young's modulus was found to increase with increasing DOPG content regardless of fabrication method. When bilayers of the same composition were fabricated using the lipid-in-aqueous method, they were found to have higher moduli. This also supports our hypothesis that the lipid-in-aqueous approach encourages the greater exclusion of oil molecules from the formed bilayer, since additional oil molecules in the membrane would result in more compressible membranes. Our results are consistent with bending modulus measurements of GUVs with varying DOPG concentration performed using optical tweezers which exhibited the same trend of increasing modulus with higher DOPG content (62).

Asymmetric Membranes From Lipid-in-aqueous Approach

To qualitatively demonstrate the formation of asymmetric membranes with independent aqueous solution conditions on either side of the bilayer, a series of quenching assays were performed. As a control, a symmetric bilayer composed of DOPC and 1 mol% DOPE-Rh (DOPC:DOPE-Rh 99:1) was formed using the lipid-in-oil approach before introducing QSY-7 to the top compartment of the bilayer. Satisfactorily, the fluorescence intensity was found to decrease by about 55% with minimal variation in fluorescence intensity within the bilayer area, indicating that one leaflet was fully quenched (Figure 5A). An asymmetric bilayer was then formed using the lipid-in-aqueous approach with DOPC vesicles on one side and DOPC:DOPE-Rh 99:1 on the other. When QSY-7 was added to the side containing no DOPE-Rh, there was a negligible change in fluorescence intensity

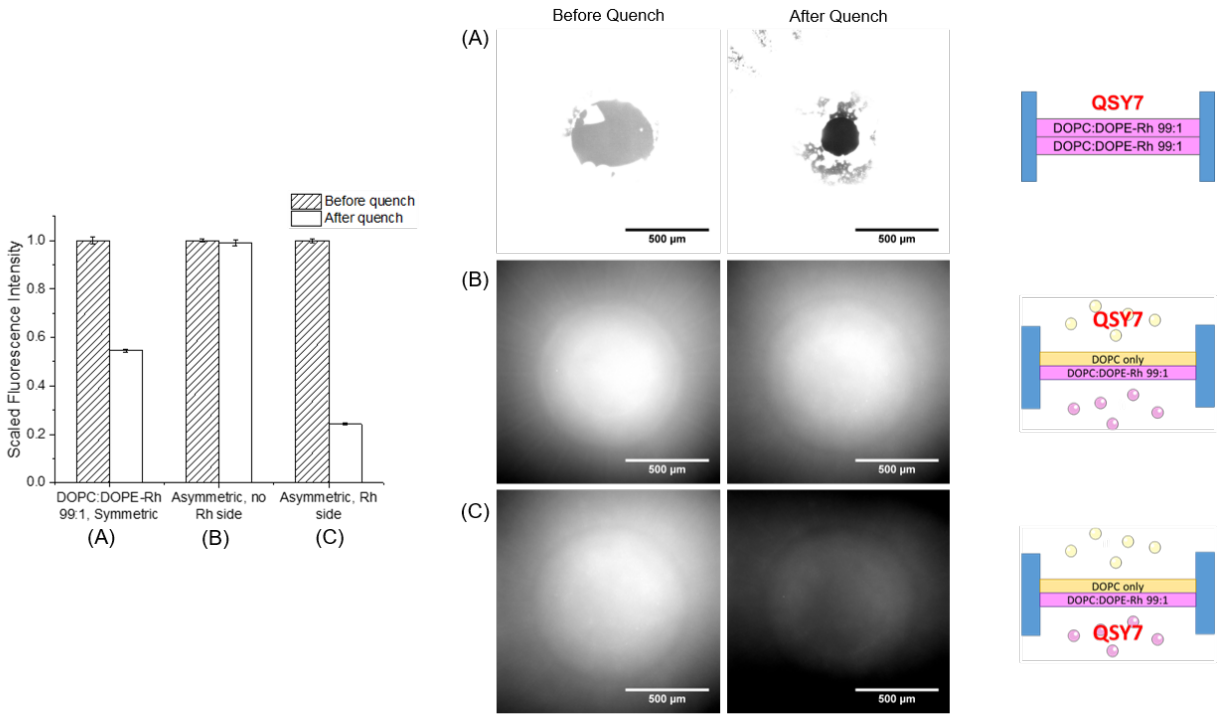

Figure 5: a) Fluorescence quenching of a symmetric DOPC membrane formed from the oil phase using QSY-7 added to one side shows the chemical isolation between the two sides of the membrane and a 50% decrease in fluorescence intensity, indicating one leaflet is fully quenched. Fluorescence quenching of an asymmetric membrane with fluorescence headgroup on only one side of the membrane shows b) no decrease in intensity when the quencher is added to the opposite side and c) a steep decrease in intensity when the quencher is added to the same side of the fluorescent headgroup.

(Figure 5B). However, when QSY-7 was added to the bottom of the asymmetric bilayer, which was the leaflet composed of DOPC:DOPE-Rh 99:1, there was about an 80% drop in fluorescence intensity, as shown in Figure 5C, with residual background fluorescence remaining.

The fluorescence experiments done to validate the lipid-in-aqeous method of generating asymmetric planar membranes bring about two conclusions. One, it is clear that the oil film separates the two components of aqueous lipids so that the asymmetric membrane can form without lipid mixing. Secondly, once the membrane is formed we do not observe lipid flip-flop within the duration of a typical experiment (~three hours). This is supported by experiments tracking lipid flip-flop in SLBs or GUVs, which have found this process occurs on the order of a half day (63). While bilayer asymmetry is not thermodynamically unstable, there is still an energy cost associated with the flip-flop mechanism, and in this case, it seems high enough that asymmetric membranes can be fabricated and interrogated within a reasonable experimental time frame.

In an asymmetrically charged bilayer, the membrane holds a charge in the absence of an applied voltage (30). This is opposed to an asymmetric bilayer with solely zwitterionic phospholipids, and a symmetric bilayer with or without charged lipids, which will all possess a net zero charge in the absence of any applied voltage. Normally when some voltage is applied to the bilayer, it will be compressed, however in the case of an asymmetrically charged bilayer, if the applied voltage is equal and opposite to the membrane charge, the membrane will actually become thicker. Experimentally, this is seen in the shift of the vertex of the quadratic fit of the thickness to voltage data. In an asymmetric bilayer fabricated on the LAMB with one leaflet of 100% DOPC and one leaflet of 50% DOPC and 50% DOPG, this offset voltage was measured to be 15 mV, which can be seen in Figure 6A and B. This shift must be taken into account in determining the membrane Young's modulus, such that

$$\Delta d = d_{V_{\text{offset}}} - d(V) = \frac{C_{m,V_{\text{offset}}}(V - V_{\text{offset}})^2}{2E_{\perp}} \tag{2}$$

where $d_{V_{\text{offset}}}$ and $C_{m,V_{\text{offset}}}$ is the thickness and specific capacitance, respectively, at the offset voltage. This shift is shown in Figure 6C, indicating that after taking the offset voltage into account the thickness data once again follow the expected voltage squared relationship, which allows for determination of the Young's modulus of asymmetric membranes.

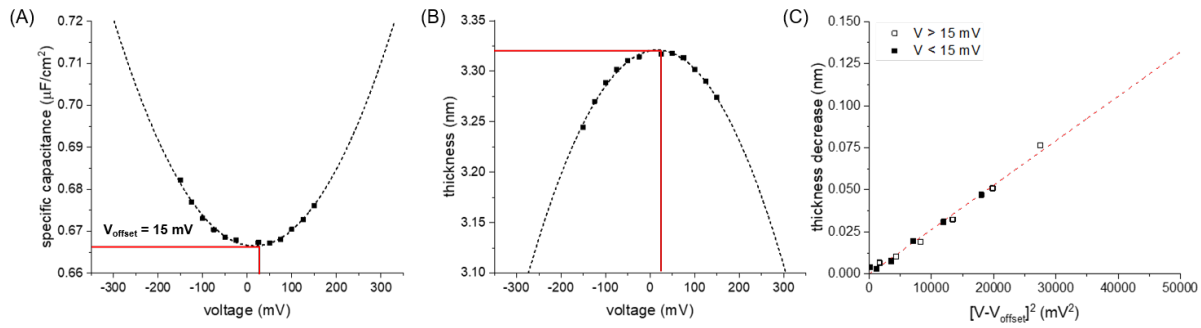

Figure 6: A) Specific capacitance and b) thickness of an asymmetric DOPC/DOPG bilayer show asymmetric compression upon voltage application. C) By considering the offset in potential caused by the charge asymmetry, the data still follow the expected V^2 dependence.

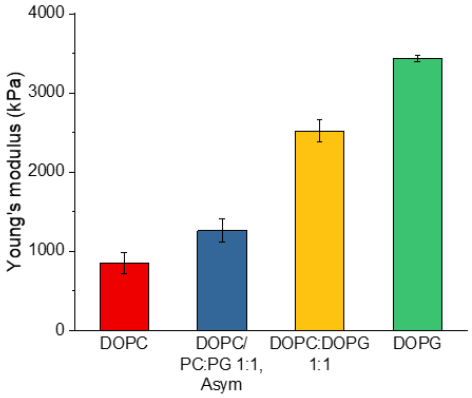

Figure 7: Membrane Young's modulus from various DOPC/DOPG bilayers formed from the lipid-in-aqueous approach.

The 1430 kPa Young's modulus of this asymmetric membrane is higher than that of the symmetric DOPC bilayer made with the lipid-in-aqueous method, but it is lower than that of the 50/50 DOPC/DOPG bilayer made via the same fabrication route. A comparison of the moduli of bilayers of different compositions formed with the lipid-in-aq bilayer is shown in Figure 7. The material properties of an asymmetric membrane are in line with what one would expect of a bilayer with higher DOPC content. The modulus of the asymmetric bilayer is between that of a symmetric DOPC and symmetric DOPC:DOPG 1:1 bilayer, which is consistent with the proportion of total DOPC contained in the asymmetric bilayer. These results demonstrate a novel improvement on the fabrication and characterization of free-standing asymmetric membranes with compositional control over both leaflets of the membrane.

CONCLUSION

The LAMB platform has been used to systematically characterize the material properties of symmetric bilayers with varying anionic phospholipid headgroup concentrations formed from the previous lipid-in-oil approach and the new lipid-in-aqueous method. The lipid-in-aqueous method allows for the fabrication of freestanding membranes with leaflet asymmetry. The effect of charged headgroups in a lipid bilayer has been quantified in terms of its effect on static thickness, modulus, and offset voltage. Increasing the concentration of charged DOPG phospholipids in the bilayer causes an increase in the static thickness and modulus of the bilayer, with the lipid-in-aqueous approach excluding more oil molecules from the formed membrane. Stable asymmetric bilayers were formed and verified qualitatively using a fluorescence quenching assay, and quantitatively verified by the detection of an offset voltage from capacitance measurements of a charge asymmetric membrane. The modulus of this asymmetric bilayer is in line with the compositional trends of the symmetric bilayers. These studies lay the groundwork for more comprehensive work involving more complex lipid mixtures with the resolution to systematically measure the effects of perturbations of composition and solution conditions on membrane material properties.

AUTHOR CONTRIBUTIONS

PJB designed the research. OZ performed and analyzed lipid-in-oil experiments. PL performed and analyzed lipid-in-aqueous experiments. All authors wrote the article.

ACKNOWLEDGMENTS

Funding for this research was provided by NSF under Award No. CBET-1942581 and the University of Massachusetts Amherst. The authors also acknowledge the UMass Institute for Applied Life Sciences AddFab facility for assistance fabricating sample cells used in this work.

REFERENCES

1. Chan, Y. H. M., and S. G. Boxer, 2007. Model membrane systems and their applications. *Current Opinion in Chemical Biology* 11:581–587.

2. Lagny, T. J., and P. Bassereau, 2015. Bioinspired membrane-based systems for a physical approach of cell organization and dynamics: usefulness and limitations. *Interface Focus* 5:20150038–20150038. http://rsfs.royalsocietypublishing.org/cgi/doi/10.1098/rsfs.2015.0038.

3. Siontorou, C., G.-P. Nikoleli, D. Nikolelis, S. Karapetis, C. G. Siontorou, G.-P. Nikoleli, D. P. Nikolelis, and S. K. Karapetis, 2017. Artificial Lipid Membranes: Past, Present, and Future. *Membranes* 7:38. http://www.mdpi.com/2077-0375/7/3/38.

4. Van Meer, G., D. R. Voelker, and G. W. Feigenson, 2008. Membrane lipids: Where they are and how they behave. *Nature Reviews Molecular Cell Biology* 9:112–124.

5. Harayama, T., and H. Riezman, 2018. Understanding the diversity of membrane lipid composition www.nature.com/nrm.

6. Walde, P., K. Cosentino, H. Engel, and P. Stano, 2010. Giant Vesicles: Preparations and Applications. *ChemBioChem* 11:848–865.

7. Rideau, E., R. Dimova, P. Schwille, F. R. Wurm, and K. Landfester, 2018. Liposomes and polymersomes: a comparative review towards cell mimicking. *Chemical Society reviews* 47:8572–8610. https://pubs.rsc.org/en/content/articlehtml/2018/cs/c8cs00162fhttps://pubs.rsc.org/en/content/articlelanding/2018/cs/c8cs00162f.

8. Bayley, H., B. Cronin, A. Heron, M. A. Holden, W. L. Hwang, R. Syeda, J. Thompson, and M. Wallace, 2008. Droplet interface bilayers. *Molecular BioSystems* 4:1191–1208. https://pubs.rsc.org/en/content/articlehtml/2008/mb/b808893dhttps://pubs.rsc.org/en/content/articlelanding/2008/mb/b808893d.

9. Leptihn, S., O. K. Castell, B. Cronin, E. H. Lee, L. C. Gross, D. P. Marshall, J. R. Thompson, M. Holden, and M. I. Wallace, 2013. Constructing droplet interface bilayers from the contact of aqueous droplets in oil. *Nature Protocols* 8:1048–1057.

10. Allen-Benton, M., H. E. Findlay, and P. J. Booth, 2019. Probing membrane protein properties using droplet interface bilayers. http://journals.sagepub.com/doi/10.1177/1535370219847939.

11. Castellana, E. T., and P. S. Cremer, 2006. Solid supported lipid bilayers: From biophysical studies to sensor design. *Surface Science Reports* 61:429–444.

12. Kurniawan, J., J. F. Ventrici De Souza, A. T. Dang, G. Y. Liu, and T. L. Kuhl, 2018. Preparation and Characterization of Solid-Supported Lipid Bilayers Formed by Langmuir-Blodgett Deposition: A Tutorial. *Langmuir* 34:15622–15639. https://pubs.acs.org/sharingguidelines.

13. Winterhalter, M., 2000. Black lipid membranes.

14. Tsemperouli, M., E. Amstad, N. Sakai, S. Matile, and K. Sugihara, 2019. Black lipid membranes: Challenges in simultaneous quantitative characterization by electrophysiology and fluorescence microscopy. *Langmuir* 35:8718–8757. https://pubs.acs.org/sharingguidelines.

15. Kwok, R., and E. Evans, 1981. Thermoelasticity of large lecithin bilayer vesicles. *Biophysical Journal* 35:637–652.

16. Rawicz, W., K. C. Olbrich, T. McIntosh, D. Needham, and E. A. Evans, 2000. Effect of chain length and unsaturation on elasticity of lipid bilayers. *Biophysical Journal* 79:328–339.

17. Döbereiner, H. G., G. Gompper, C. K. Haluska, D. M. Kroll, P. G. Petrov, and K. A. Riske, 2003. Advanced Flicker Spectroscopy of Fluid Membranes. *Physical Review Letters* 91:048301. https://journals.aps.org/prl/abstract/10.1103/PhysRevLett.91.048301.

18. Rautu, S. A., D. Orsi, L. Di Michele, G. Rowlands, P. Cicuta, and M. S. Turner, 2017. The role of optical projection in the analysis of membrane fluctuations. *Soft Matter* 13:3480–3483. http://xlink.rsc.org/?DOI=C7SM00108H.

19. Daillant, J., E. Bellet-Amalric, A. Braslau, T. Charitat, G. Fragneto, F. Graner, S. Mora, F. Rieutord, and B. Stidder, 2005. Structure and fluctuations of a single floating lipid bilayer. *Proceedings of the National Academy of Sciences* 102:11639–11644. http://www.pnas.org/cgi/doi/10.1073/pnas.0504588102.

20. Hemmerle, A., L. Malaquin, T. Charitat, S. Lecuyer, G. Fragneto, and J. Daillant, 2012. Controlling interactions in supported bilayers from weak electrostatic repulsion to high osmotic pressure. *Proceedings of the National Academy of Sciences* 109:19938–19942. http://www.pnas.org/cgi/doi/10.1073/pnas.1211669109.

21. Gross, L. C., A. J. Heron, S. C. Baca, and M. I. Wallace, 2011. Determining membrane capacitance by dynamic control of droplet interface bilayer area. *Langmuir* 27:14335–14342. https://pubs.acs.org/sharingguidelines.

22. White, S. H., and W. Chang, 1981. Voltage dependence of the capacitance and area of black lipid membranes. *Biophysical Journal* 36:449–453.

23. Hianik, T., J. Dlugopolsky, and M. Gyepessova, 1993. Electrostriction of lipid bilayers on a solid support. Influence of hydrocarbon solvent and d.c. voltage. *Bioelectrochemistry and Bioenergetics* 31:99–111. https://www.sciencedirect.com/science/article/pii/030245989386109E.

24. Hianik, T., J. Dlugopolsky, V. Passechnik, D. Sargent, and S. Ivanov, 1996. Electrostriction and membrane potential of lipid bilayers on a metal support. *Colloids and Surfaces A: Physicochemical and Engineering Aspects* 106:109–118. https://www.sciencedirect.com/science/article/pii/0927775795033823.

25. Bretscher, M. S., 1972. Asymmetrical Lipid Bilayer Structure for Biological Membranes. *Nature New Biology* 236:11–12. http://link.springer.com/10.1038/newbio236011a0.

26. Verkleij, A., R. Zwaal, B. Roelofsen, P. Comfurius, D. Kastelijn, and L. van Deenen, 1973. The asymmetric distribution of phospholipids in the human red cell membrane. A combined study using phospholipases and freeze-etch electron microscopy. *Biochimica et Biophysica Acta (BBA) - Biomembranes* 323:178–193. https://www.sciencedirect.com/science/article/pii/0005273673901430?via{%}3Dihub.

27. Alvarez, O., and R. Latorre, 1978. Voltage-dependent capacitance in lipid bilayers made from monolayers. *Biophysical Journal* 21:1–17. http://dx.doi.org/10.1016/S0006-3495(78)85505-2.

28. Op den Kamp, J. A. F., 1979. Lipid Asymmetry in Membranes. *Annual Review of Biochemistry* 48:47–71. http://www.annualreviews.org/doi/10.1146/annurev.bi.48.070179.000403.

29. Boon, J. M., and B. D. Smith, 2002. Chemical control of phospholipid distribution across bilayer membranes. *Medicinal research reviews* 22:251–81. http://www.ncbi.nlm.nih.gov/pubmed/11933020.

30. Mosgaard, L. D., K. A. Zecchi, T. Heimburg, and R. Budvytyte, 2015. The effect of the nonlinearity of the response of lipid membranes to voltage perturbations on the interpretation of their electrical properties. A new theoretical description. *Membranes* 5:495–512.

31. Langner, M., and K. Kubica, 1999. The electrostatics of lipid surfaces. *Chemistry and Physics of Lipids* 101:3–35. https://linkinghub.elsevier.com/retrieve/pii/S0009308499000523.

32. Pomorski, T., R. Lombardi, H. Riezman, P. F. Devaux, G. van Meer, and J. C. M. Holthuis, 2003. Drs2p-related P-type ATPases Dnf1p and Dnf2p Are Required for Phospholipid Translocation across the Yeast Plasma Membrane and Serve a Role in Endocytosis. *Molecular Biology of the Cell* 14:1240–1254. http://www.molbiolcell.org/doi/10.1091/mbc.e02-08-0501.

33. Pliotas, C., A. C. E. Dahl, T. Rasmussen, K. R. Mahendran, T. K. Smith, P. Marius, J. Gault, T. Banda, A. Rasmussen, S. Miller, C. V. Robinson, H. Bayley, M. S. Sansom, I. R. Booth, and J. H. Naismith, 2015. The role of lipids in mechanosensation. *Nature Structural and Molecular Biology* 22:991–998. http://dx.doi.org/10.1038/nsmb.3120.

34. Brohawn, S. G., E. B. Campbell, and R. MacKinnon, 2014. Physical mechanism for gating and mechanosensitivity of the human TRAAK K+ channel. *Nature* 516:126–130. http://dx.doi.org/10.1038/nature14013.

35. Deliconstantinos, G., 1987. Physiological aspects of membrane lipid fluidity in malignancy. https://europepmc.org/article/med/3324933.

36. Ran, S., A. Downes, and P. E. Thorpe, 2002. Increased exposure of anionic phospholipids on the surface of tumor blood vessels. *Cancer research* 62:6132–40. http://www.ncbi.nlm.nih.gov/pubmed/12414638.

37. Szachowicz-Petelska, B., I. Dobrzyńska, M. Skrodzka, B. Darewicz, Z. A. Figaszewski, and J. Kudelski, 2013. Phospholipid composition and electric charge in healthy and cancerous parts of human kidneys. *The Journal of membrane biology* 246:421–5. http://www.ncbi.nlm.nih.gov/pubmed/23649039http://www.pubmedcentral.nih.gov/articlerender.fcgi?artid=PMC3654190.

38. Dobrzyńska, I., B. Szachowicz-Petelska, B. Darewicz, and Z. A. Figaszewski, 2015. Characterization of human bladder cell membrane during cancer transformation. *The Journal of membrane biology* 248:301–7. http://www.ncbi.nlm.nih.gov/pubmed/25572835http://www.pubmedcentral.nih.gov/articlerender.fcgi?artid=PMC4381039.

39. Alves, A. C., D. Ribeiro, C. Nunes, and S. Reis, 2016. Biophysics in cancer: The relevance of drug-membrane interaction studies. *Biochimica et Biophysica Acta - Biomembranes* 1858:2231–2244. http://dx.doi.org/10.1016/j.bbamem.2016.06.025.

40. Perrotti, F., C. Rosa, I. Cicalini, P. Sacchetta, P. Del Boccio, D. Genovesi, and D. Pieragostino, 2016. Advances in lipidomics for cancer biomarkers discovery. https://pubmed.ncbi.nlm.nih.gov/27916803/.

41. Liu, L. K., V. Choudhary, A. Toulmay, and W. A. Prinz, 2017. An inducible ER-Golgi tether facilitates ceramide transport to alleviate lipotoxicity. *Journal of Cell Biology* 216:131–147. https://doi.org/10.1083/jcb.201606059.

42. Sharma, B., and S. S. Kanwar, 2018. Phosphatidylserine: A cancer cell targeting biomarker.

43. Cheng, H.-T., Megha, and E. London, 2009. Preparation and properties of asymmetric vesicles that mimic cell membranes: effect upon lipid raft formation and transmembrane helix orientation. *The Journal of biological chemistry* 284:6079–92. http://www.ncbi.nlm.nih.gov/pubmed/19129198http://www.pubmedcentral.nih.gov/articlerender.fcgi?artid=PMC2649079.

44. Doktorova, M., F. A. Heberle, B. Eicher, R. F. Standaert, J. Katsaras, E. London, G. Pabst, and D. Marquardt, 2018. Preparation of asymmetric phospholipid vesicles for use as cell membrane models. *Nature Protocols* 1. http://www.nature.com/articles/s41596-018-0033-6.

45. Pautot, S., B. J. Frisken, and D. A. Weitz, 2003. Engineering asymmetric vesicles. *Proceedings of the National Academy of Sciences of the United States of America* 100:10718–21. http://www.ncbi.nlm.nih.gov/pubmed/12963816http://www.pubmedcentral.nih.gov/articlerender.fcgi?artid=PMC196870.

46. Arriaga, L. R., Y. Huang, S.-H. Kim, J. L. Aragones, R. Ziblat, S. A. Koehler, and D. A. Weitz, 2019. Single-step assembly of asymmetric vesicles. *Lab on a Chip* 19:749–756. http://xlink.rsc.org/?DOI=C8LC00882E.

47. Kamiya, K., R. Kawano, T. Osaki, K. Akiyoshi, and S. Takeuchi, 2016. Cell-sized asymmetric lipid vesicles facilitate the investigation of asymmetric membranes. *Nature Chemistry* 8:881–889.

48. Lin, W. C., C. D. Blanchette, T. V. Ratto, and M. L. Longo, 2006. Lipid asymmetry in DLPC/DSPC-supported lipid bilayers: A combined AFM and fluorescence microscopy study. *Biophysical Journal* 90:228–237. /pmc/articles/PMC1367021/?report=abstracthttps://www.ncbi.nlm.nih.gov/pmc/articles/PMC1367021/.

49. Kiessling, V., C. Wan, and L. K. Tamm, 2009. Domain coupling in asymmetric lipid bilayers.

50. Visco, I., S. Chiantia, and P. Schwille, 2014. Asymmetric supported lipid bilayer formation via methyl-β-cyclodextrin mediated lipid exchange: Influence of asymmetry on lipid dynamics and phase behavior. *Langmuir* 30:7475–7484. https://pubs.acs.org/doi/abs/10.1021/la500468r.

51. Hwang, W. L., M. Chen, B. Cronin, M. A. Holden, and H. Bayley, 2008. Asymmetric droplet interface bilayers. *Journal of the American Chemical Society* 130:5878–5879.

52. Milianta, P. J., M. Muzzio, J. Denver, G. Cawley, and S. Lee, 2015. Water permeability across symmetric and asymmetric droplet interface bilayers: Interaction of cholesterol sulfate with DPhPC. *Langmuir* 31:12187–12196.

53. Gutsmann, T., T. Heimburg, U. Keyser, K. R. Mahendran, and M. Winterhalter, 2015. Protein reconstitution into freestanding planar lipid membranes for electrophysiological characterization. *Nature Protocols* 10:188–198.

54. Lu, L., W. J. Doak, J. W. Schertzer, and P. R. Chiarot, 2016. Membrane mechanical properties of synthetic asymmetric phospholipid vesicles. *Soft Matter* 12:7521–7528. http://xlink.rsc.org/?DOI=C6SM01349J.

55. Karamdad, K., R. V. Law, J. M. Seddon, N. J. Brooks, and O. Ces, 2016. Studying the effects of asymmetry on the bending rigidity of lipid membranes formed by microfluidics. *Chem. Commun.* 52:5277–5280. http://xlink.rsc.org/?DOI=C5CC10307J.

56. Beltramo, P. J., R. Van Hooghten, and J. Vermant, 2016. Millimeter-area, free standing, phospholipid bilayers. *Soft Matter* 12:4324–4331. http://xlink.rsc.org/?DOI=C6SM00250A.

57. Beltramo, P. J., L. Scheidegger, and J. Vermant, 2018. Toward Realistic Large-Area Cell Membrane Mimics: Excluding Oil, Controlling Composition, and Including Ion Channels. *Langmuir* 34:5880–5888. http://pubs.acs.org/doi/10.1021/acs.langmuir.8b00837https://doi.org/10.1021/acs.langmuir.8b00837.

58. Beltramo, P. J., and J. Vermant, 2016. Simple Optical Imaging of Nanoscale Features in Free-Standing Films. *ACS Omega* 1:363–370. http://gateway.webofknowledge.com/gateway/Gateway.cgi?GWVersion=2{&}SrcAuth=ORCID{&}SrcApp=OrcidOrg{&}DestLinkType=FullRecord{&}DestApp=WOS{_}CPL{&}KeyUT=WOS:000391204000006{&}KeyUID=WOS:000391204000006.

59. Ardham, V. R., V. Zoni, S. Adamowicz, P. Campomanes, and S. Vanni, 2020. Accurate Estimation of Membrane Capacitance from Atomistic Molecular Dynamics Simulations of Zwitterionic Lipid Bilayers. *The Journal of Physical Chemistry B* 2020:8286. https://dx.doi.org/10.1021/acs.jpcb.0c03145.

60. Kučerka, N., S. Tristram-Nagle, and J. F. Nagle, 2006. Structure of fully hydrated fluid phase lipid bilayers with monounsaturated chains. *Journal of Membrane Biology* 208:193–202.

61. Kučerka, N., M. P. Nieh, and J. Katsaras, 2011. Fluid phase lipid areas and bilayer thicknesses of commonly used phosphatidylcholines as a function of temperature. *Biochimica et Biophysica Acta - Biomembranes* 1808:2761–2771.

62. Shitamichi, Y., M. Ichikawa, and Y. Kimura, 2009. Mechanical properties of a giant liposome studied using optical tweezers. *Chemical Physics Letters* 479:274–278.

63. Devaux, P. F., P. Fellmann, and P. Hervé, 2002. Investigation on lipid asymmetry using lipid probes: Comparison between spin-labeled lipids and fluorescent lipids. *Chemistry and Physics of Lipids* 116:115–134. https://pubmed.ncbi.nlm.nih.gov/12093538/.

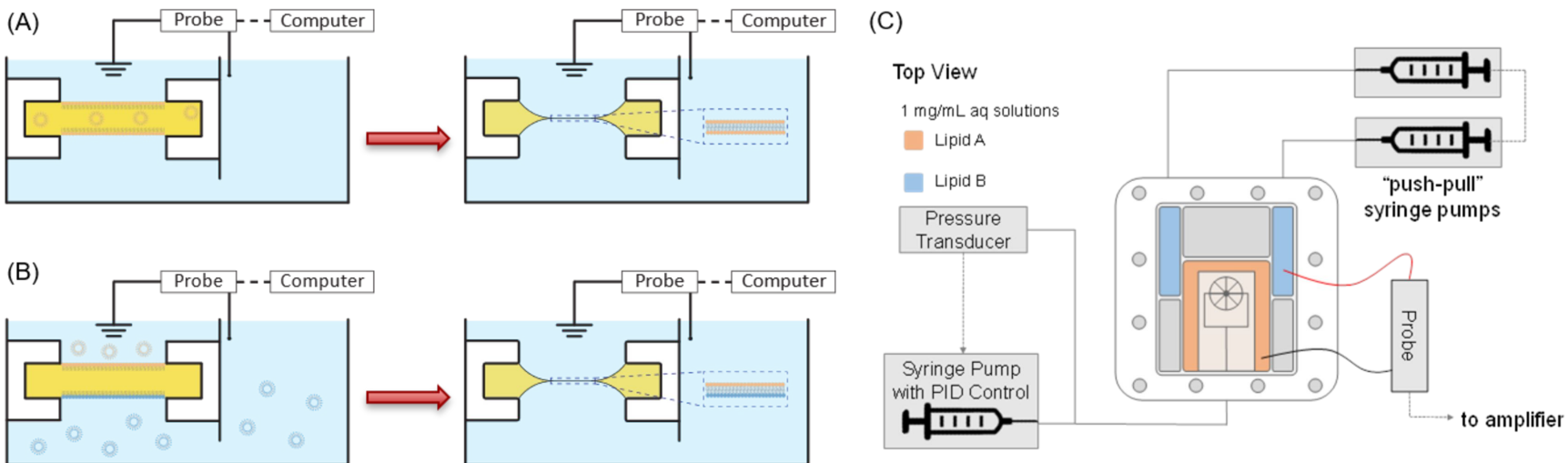
(A)
Probe
Computer
Probe
Computer
(B)
Probe
Computer
Probe
Computer
(C)
Top View
1 mg/mL aq solutions
Lipid A
Lipid B
Pressure Transducer
Syringe Pump with PID Control
"push-pull" syringe pumps
Probe
to amplifier

(A)

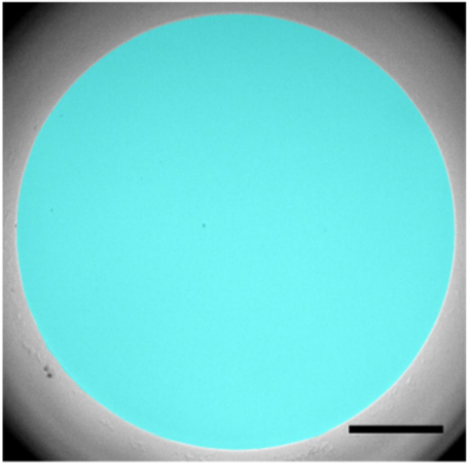

(B)

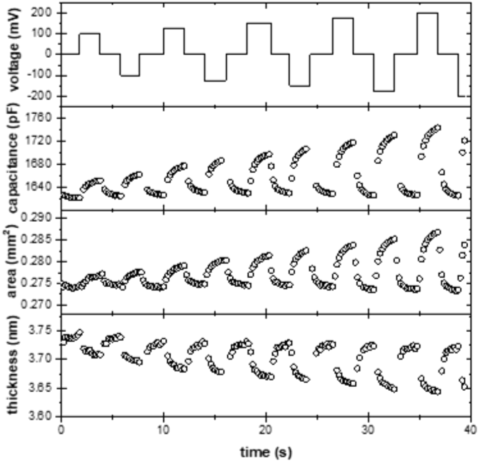
voltage (mV)
200
100
0
-100
-200
capacitance (pF)
1760
1720
1680
1640
area (mm²)
0.290
0.285
0.280
0.275
0.270
thickness (nm)
3.75
3.70
3.65
3.60
0
10
20
30
40
time (s)

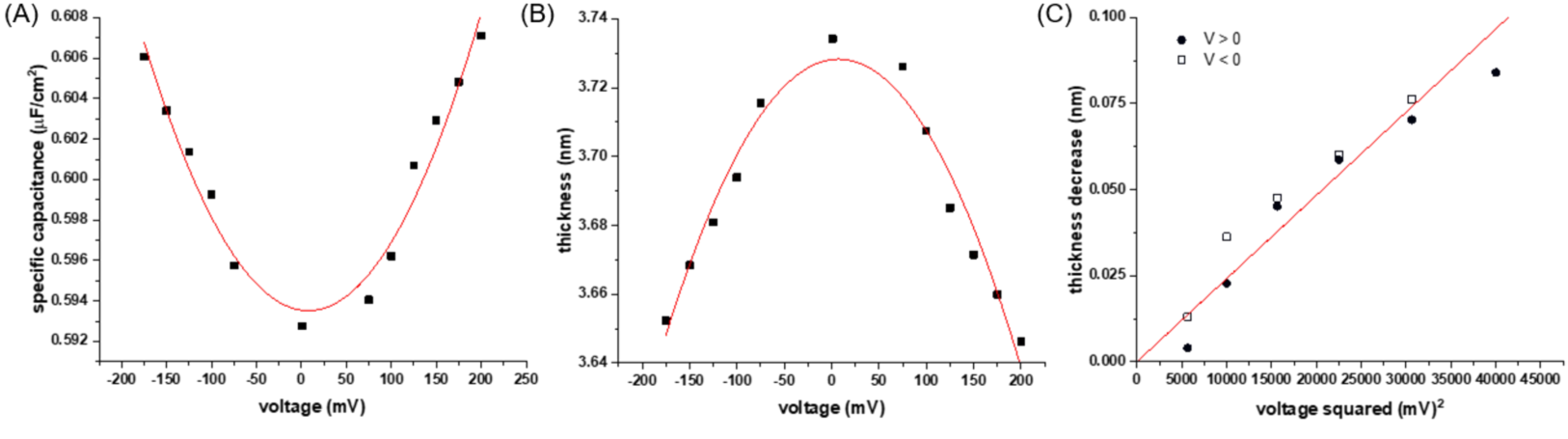
(A)
specific capacitance (μF/cm²)
0.608
0.606
0.604
0.602
0.600
0.598
0.596
0.594
0.592
-200 -150 -100 -50 0 50 100 150 200 250
voltage (mV)
(B)
thickness (nm)
3.74
3.72
3.70
3.68
3.66
3.64
-200 -150 -100 -50 0 50 100 150 200
voltage (mV)
(C)
V > 0
V < 0
thickness decrease (nm)
0.100
0.075
0.050
0.025
0.000
0 5000 10000 15000 20000 25000 30000 35000 40000 45000
voltage squared (mV)²

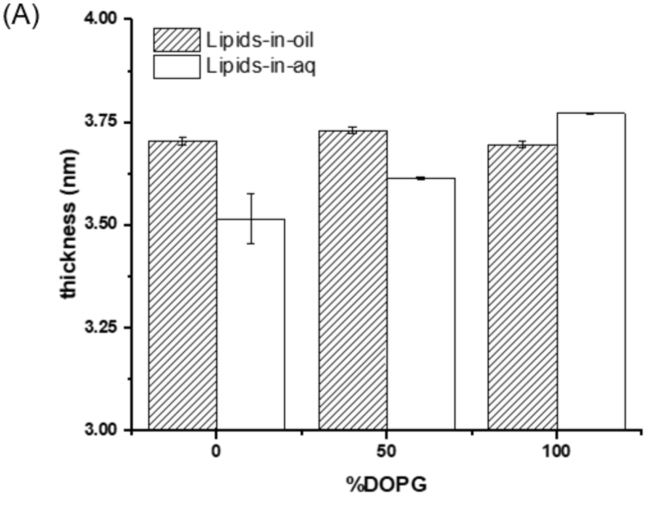
(A)
Lipids-in-oil
Lipids-in-aq
thickness (nm)
4.00
3.75
3.50
3.25
3.00
0
50
100
%DOPG

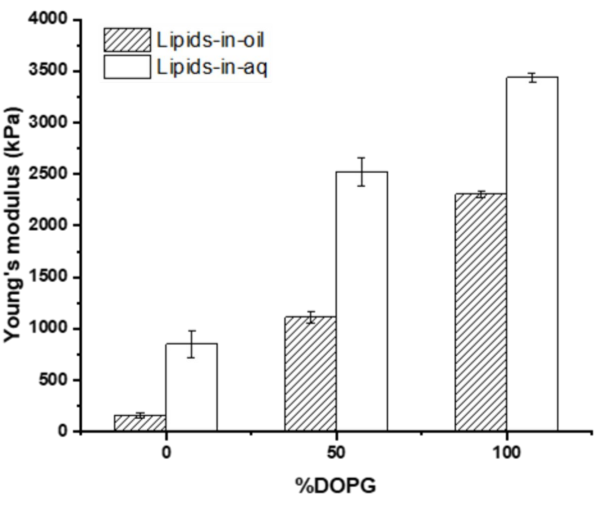
(B)
Lipids-in-oil
Lipids-in-aq
Young's modulus (kPa)
4000
3500
3000
2500
2000
1500
1000
500
0
0
50
100
%DOPG

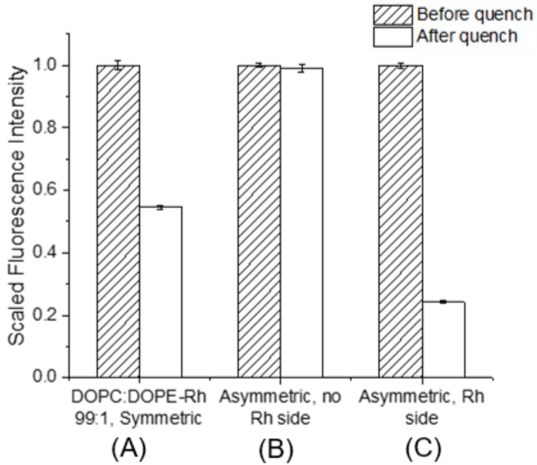
Before quench
After quench
Scaled Fluorescence Intensity
1.0
0.8
0.6
0.4
0.2
0.0
DOPC:DOPE-Rh 99:1, Symmetric
Asymmetric, no Rh side
Asymmetric, Rh side
(A)
(B)
(C)

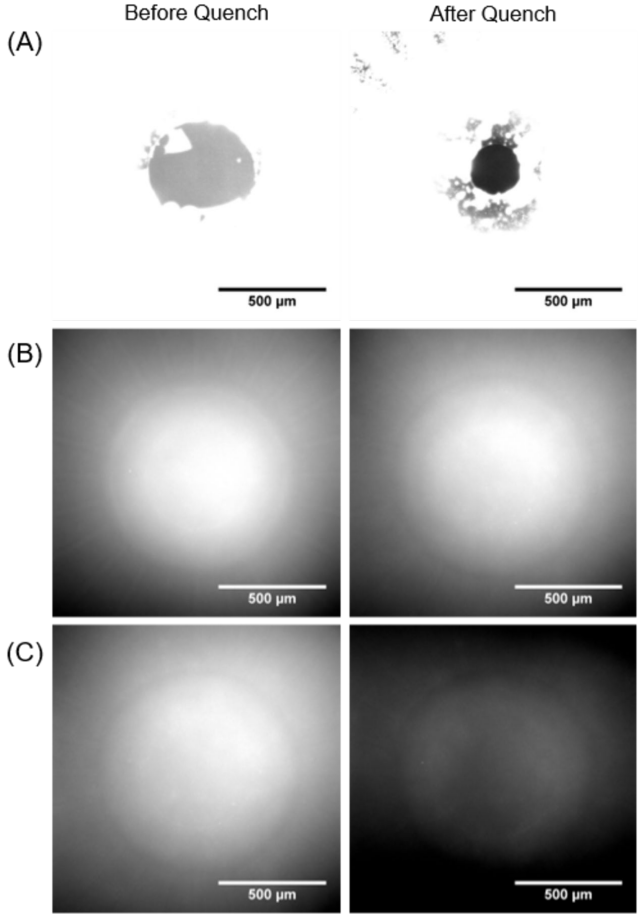
Before Quench
After Quench
(A)
500 µm
500 µm
(B)
500 µm
500 µm
(C)
500 µm
500 µm

QSY7
DOPC:DOPE-Rh 99:1
DOPC:DOPE-Rh 99:1
QSY7
DOPC only
DOPC:DOPE-Rh 99:1
DOPC only
DOPC:DOPE-Rh 99:1
QSY7

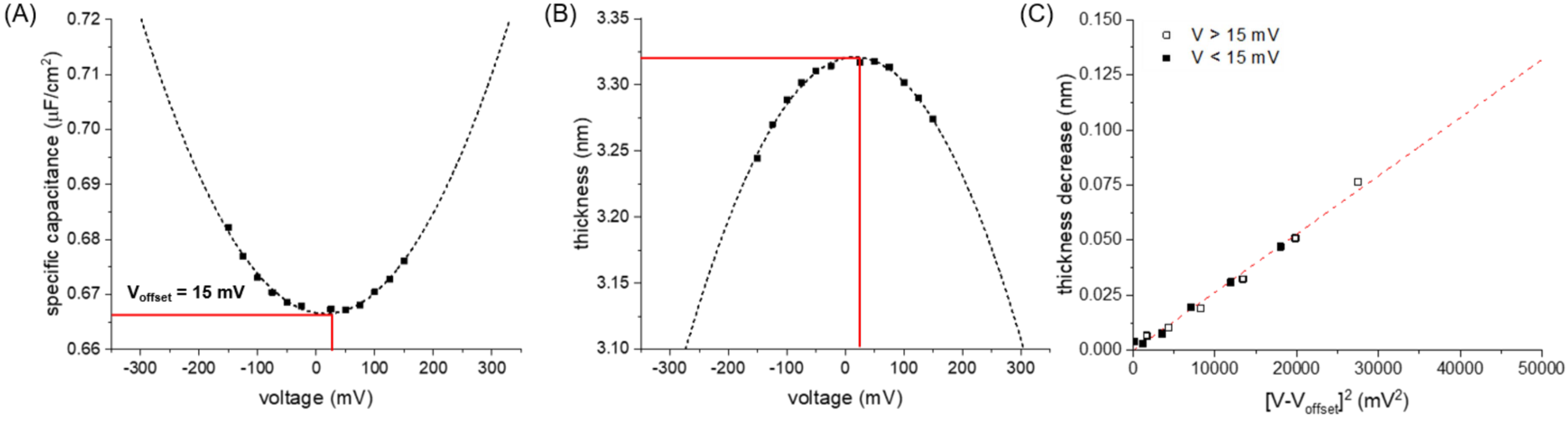
(A)
specific capacitance (μF/cm²)
0.72
0.71
0.70
0.69
0.68
0.67
0.66
V_offset = 15 mV
-300
-200
-100
0
100
200
300
voltage (mV)
(B)
thickness (nm)
3.35
3.30
3.25
3.20
3.15
3.10
-300
-200
-100
0
100
200
300
voltage (mV)
(C)
V > 15 mV
V < 15 mV
thickness decrease (nm)
0.150
0.125
0.100
0.075
0.050
0.025
0.000
0
10000
20000
30000
40000
50000
[V-V_offset]² (mV²)

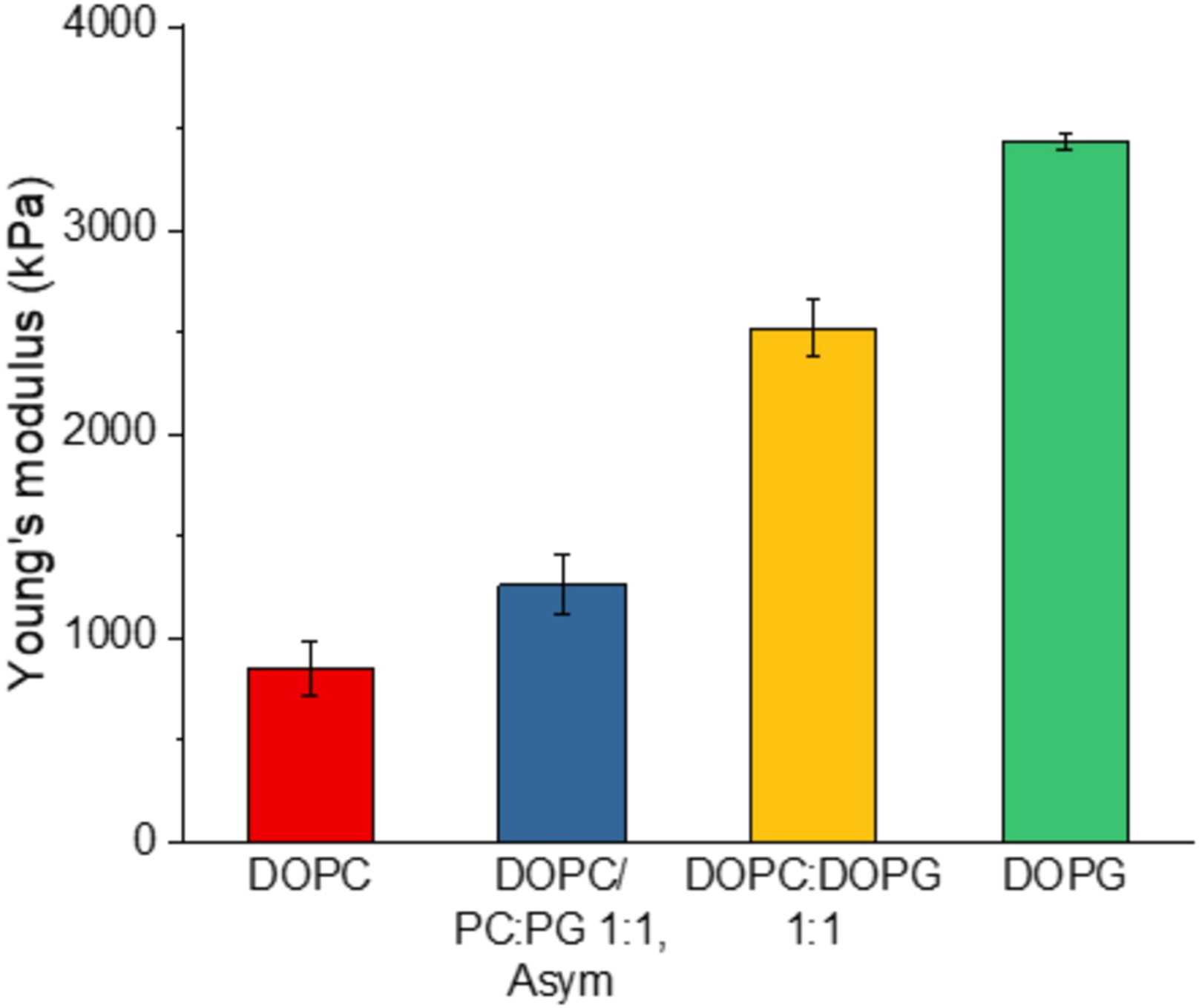
Young's modulus (kPa)
4000
3000
2000
1000
0
DOPC
DOPC/
PC:PG 1:1,
Asym
DOPC:DOPG
1:1
DOPG